2007 IEEE International Conference on
Robotics and Automation
Roma, Italy, 10-14 April 2007

A Transparent Bilateral Controller for Teleoperation Considering the Transition of Motion

Heng Wang*, K. H. Low*, and Michael Yu Wang†
*School of Mechanical and Aerospace Engineering
Nanyang Technological University, Singapore 639798
wh@pmail.ntu.edu.sg, mkhlow@ntu.edu.sg
†Department of Mechanical and Automation Engineering
The Chinese University of Hong Kong, Hong Kong, China
yuwang@mae.cuhk.edu.hk

***Abstract*— A two-channel bilateral controller is proposed for teleoperation systems, which takes into account both the free space motion and the constrained motion. Specifically, the force-position (F-P) architecture is applied during the constrained motion, while the position-position (P-P) architecture is applied during the free space motion. Perfect transparency can be achieved in theory. In addition, the controller is robust to model uncertainties and disturbances, and it does not need to switch the control modes of the master and the slave controllers during the transition between the free space motion and the constrained motion. Experiments are conducted to demonstrate the effectiveness of the proposed bilateral controller.**

I. Introduction

The major objective in designing the teleoperation control system is to achieve transparency provided that the system is stable. That is, both the position and the force at the master and the slave are well matched.

Based on the four-channel architecture developed by Lawrence [1], Hashtrudi-Zaad and Salcudean [2] have shown that only three data channels can result in perfect transparency by employing local force feedback. Recently, by analyzing the four-channel architecture with local force feedback, Kim, *et al.* [3] showed that perfect transparency can be achieved in the position-force (P-F) and force-position (F-P) two-channel architectures. Note that in this paper, the P-F architecture is the system, in which the position information is sent from the master to the slave, and the force information is sent from the slave to the master. This result conforms to the observations by Fite, *et al.* [4], [5], in which the authors addressed the transparency and stability of the P-F two-channel system from a frequency domain loop-shaping perspective. It was shown that the transparency and the stability robustness can be simultaneously improved in a teleoperation system, which contradicts the previous result that stability and transparency are conflicting design objectives.

Most tasks include both the unconstrained motion and the constrained motion. Previous work mainly focuses on the constrained motion without considering the transition between the unconstrained and the constrained motions. In general, the teleopeartion controllers are different in free space and in constrained condition. It is desired to have a single control law for both the constrained and unconstrained motions without switch of control modes. The force/moment accommodation (FMA) technique is applied in teleoperation systems [6]–[8], in which the control mode switch is not required during the transition of motion. However, the transparency is not considered in these work.

In our previous work, a combined impedance/direct control structure was proposed for single manipulator control [11]. Considering the transition of motion, a two-channel bilateral controller is proposed in the present work by applying the combined impedance/direct control. Perfect transparency can be achieved in theory. In addition, no control mode switch is required during the transition of motion, and the controller is robust to model uncertainties and disturbances.

In the following, the combined impedance/direct control is first reviewed. Next, the master and slave controllers are proposed, and the problem of transition of motion is addressed. Afterwards, the experimental results are presented to verify the analysis. Finally, concluding remarks are drawn.

II. Review of Combined Impedance/Direct Control

The combined impedance/direct controller is formulated based on the torque-based impedance controller. Considering only the translational motion of the end-effector, the dynamic equation of a general manipulator can be expressed in Cartesian space as

$$\mathbf{D}_x(\mathbf{q})\ddot{\mathbf{X}} + \mathbf{H}_x(\mathbf{q}, \dot{\mathbf{q}}) = \mathbf{F} - \mathbf{F}_e + \mathbf{F}_{dist} \tag{1}$$

where $\mathbf{X} \in \mathbb{R}^3$ is the robot Cartesian position, $\mathbf{q} \in \mathbb{R}^n$ denotes the joint angles, $\mathbf{D}_x(\mathbf{q}) \in \mathbb{R}^{3\times3}$ is the Cartesian inertia matrix, $\mathbf{H}_x(\mathbf{q}, \dot{\mathbf{q}}) \in \mathbb{R}^3$ includes the terms of Cartesian Coriolis and centrifugal force, and the Cartesian gravitational force, $\mathbf{F}_e \in \mathbb{R}^3$ is the force exerted by the end-effector to the environment, $\mathbf{F}_{dist} \in \mathbb{R}^3$ denotes the external disturbance force acted on the end-effector, and $\mathbf{F} \in \mathbb{R}^3$ is the control input.

Let $\mathbf{X}_r$ represent the reference trajectory, and the positive definite diagonal matrices $\mathbf{M}_t, \mathbf{B}_t, \mathbf{K}_t \in \mathbb{R}^{3\times3}$ denote the target inertia, damping, and stiffness, respectively. By defining the target impedance as

$$\mathbf{M}_t\ddot{\mathbf{E}}_x + \mathbf{B}_t\dot{\mathbf{E}}_x + \mathbf{K}_t\mathbf{E}_x = \mathbf{F}_e \tag{2}$$

where

$$\mathbf{E}_x = \mathbf{X}_r - \mathbf{X} \tag{3}$$

the typical torque-based impedance control law is then expressed as

$$\mathbf{F} = \hat{\mathbf{D}}_x \mathbf{U} + \hat{\mathbf{H}}_x + \mathbf{F}_e \tag{4}$$

where $\hat{\mathbf{D}}_x$ and $\hat{\mathbf{H}}_x$ are the estimates of $\mathbf{D}_x$ and $\mathbf{H}_x$, respectively, and

$$\mathbf{U} = \ddot{\mathbf{X}}_r + \mathbf{M}_t^{-1}(\mathbf{B}_t \dot{\mathbf{E}}_x + \mathbf{K}_t \mathbf{E}_x - \mathbf{F}_e) \tag{5}$$

By assuming that the environment can be modeled as a linear mass-damper-spring system, $\mathbf{X}_r$ in the constrained condition can be designed as [9]

$$\mathbf{X}_r = \mathbf{X}_{eo} + \mathbf{K}_{eq}^{-1} \mathbf{F}_d \tag{6}$$

where $\mathbf{X}_{eo} \in \mathbb{R}^3$ is the initial environment position without contacting the end-effector, $\mathbf{F}_d \in \mathbb{R}^3$ is the desired force, and

$$\mathbf{K}_{eq} = \mathbf{K}_t (\mathbf{K}_e + \mathbf{K}_t)^{-1} \mathbf{K}_e \tag{7}$$

with $\mathbf{K}_e \in \mathbb{R}^{3\times3}$ representing the diagonal environment stiffness matrix. It has been shown in [10] that with the presence of un-predicable disturbances, the performance of impedance control cannot be guaranteed. Based on the analysis of the closed-loop system equation, the combined impedance/direct controller was proposed as [11]

$$\mathbf{F} = \hat{\mathbf{D}}_x \left(\mathbf{U} + \mathbf{K}_p \mathbf{E}_f + \mathbf{K}_i \int_0^t \mathbf{E}_f dt \right) + \hat{\mathbf{H}}_x + \mathbf{F}_e \tag{8}$$

where $\mathbf{K}_p$ and $\mathbf{K}_i \in \mathbb{R}^{3\times3}$ are diagonal matrices, and

$$\mathbf{E}_f = \mathbf{F}_d - \mathbf{F}_e \tag{9}$$

Note that the integration term in (8) should be carefully considered, if *t* is large.

The combined impedance/direct controller combines the advantages of both the impedance control and the direct force control. Firstly, the model uncertainties and the external disturbances are handled directly, which is the advantage of the direct force control. Secondly, it does not need to switch the control modes when the end-effector transfers between the unconstrained motion and the constrained motion, which is the advantage of the impedance control. In the next section, the combined impedance/direct control is applied to design the bilateral controllers in constrained motion.

III. Bilateral Controller Design

A. Controller Design in Constrained Motion

In the constrained motion, controlling the interaction force between the slave and the environment is usually more important than the position. the F-P architecture is employed in the constrained bilateral controller, where the force information is transmitted from the master to the slave, and the position information is transmitted from the slave to the master. Specifically, the combined impedance/direct control scheme is applied on the slave, while a position control scheme with local force compensation is employed on the master.

Recall the robot dynamic equation (1), without considering the external disturbance, the master and slave dynamics are modeled as

$$\mathbf{F}_{mc} = \mathbf{D}_{xm} \ddot{\mathbf{X}}_m + \mathbf{H}_{xm} - \mathbf{F}_h \tag{10}$$

$$\mathbf{F}_{sc} = \mathbf{D}_{xs} \ddot{\mathbf{X}}_s + \mathbf{H}_{xs} + \mathbf{F}_e \tag{11}$$

where $\mathbf{D}_{xm}$ and $\mathbf{D}_{xs}$ respectively represent the master and slave inertia matrices; $\mathbf{H}_{xm}$ and $\mathbf{H}_{xs}$ respectively denote the master and slave terms corresponding to $\mathbf{H}_x$ in (1); $\mathbf{X}_m$ and $\mathbf{X}_s$ are the master and slave positions; $\mathbf{F}_h$ and $\mathbf{F}_e$ are respectively the force exerted on the master by the operator, and the force applied on the environment by the slave; and $\mathbf{F}_{mc}$ and $\mathbf{F}_{sc}$ denote the control inputs of the master and the slave, respectively.

The environment is modeled as a linear time invariant (LTI) mass-damper-spring system, which is expressed in frequency domain as

$$\mathbf{F}_e(s) = \left(\mathbf{M}_e s^2 + \mathbf{B}_e s + \mathbf{K}_e \right) \left(\mathbf{X}_s(s) - \mathbf{X}_{eo}(s) \right) \tag{12}$$

where $\mathbf{M}_e$, $\mathbf{B}_e$, and $\mathbf{K}_e \in \mathbb{R}^{3\times3}$ are the diagonal matrices representing the environment mass, damping, and stiffness coefficients, respectively. The operator dynamics is also modeled as LTI mass-damper-spring system, which is expressed in frequency domain as

$$\mathbf{F}_h(s) = \mathbf{F}_h^*(s) - \mathbf{Z}_h \mathbf{V}_h(s) \tag{13}$$

where $\mathbf{X}_h = \mathbf{X}_m$ is the human position, $\mathbf{F}_h^*$ is the operator exogenous input force, and $\mathbf{Z}_h$ denotes the operator impedance matrix, which is defined as

$$\mathbf{Z}_h = \mathbf{M}_h s + \mathbf{B}_h + \frac{\mathbf{K}_h}{s} \tag{14}$$

with $\mathbf{M}_h$, $\mathbf{B}_h$, and $\mathbf{K}_h \in \mathbb{R}^{3\times3}$ representing the operator mass, damping, and stiffness matrices, respectively.

In the constrained motion, we have $\mathbf{F}_{ed} = \mathbf{F}_h$, where $\mathbf{F}_{ed}$ denotes the desired force applied on the environment by the slave robot. According to the combined impedance/direct controller represented by (8), the following controller is proposed for the slave

$$\mathbf{F}_{sc} = \mathbf{D}_{xs} \left(\mathbf{U}_s + \mathbf{K}_{ps} \mathbf{E}_{fs} + \mathbf{K}_{is} \int_0^t \mathbf{E}_{fs} dt \right) + \mathbf{H}_{xs} + \mathbf{F}_e \tag{15}$$

where

$$\mathbf{E}_{fs} = \mathbf{F}_h - \mathbf{F}_e \tag{16}$$

$$\mathbf{U}_s = \mathbf{M}_{ts}^{-1}(\mathbf{B}_{ts}\dot{\mathbf{E}}_{xs} + \mathbf{K}_{ts}\mathbf{E}_{xs} - \mathbf{F}_e) \tag{17}$$

$$\mathbf{E}_{xs} = \mathbf{X}_{rs} - \mathbf{X}_s \tag{18}$$

$$\mathbf{X}_{rs} = \mathbf{X}_{eo} + \mathbf{K}_e^{-1}(\mathbf{K}_e + \mathbf{K}_{ts})\mathbf{K}_{ts}^{-1}\mathbf{F}_h \tag{19}$$

The nomenclature is basically the same as that defined in Sec. II, with the adding letter *s* in the subscript representing the *slave*.

For the master, we have $\mathbf{X}_{md} = \mathbf{X}_s$, where $\mathbf{X}_{md}$ is the desired master position. A position error based controller with local force compensation is employed, which is

$$\mathbf{F}_{mc} = \mathbf{D}_{xm}\Big[\ddot{\mathbf{X}}_s + \mathbf{K}_{vm}\dot{\mathbf{E}}_{ms} + \mathbf{K}_{pm}\mathbf{E}_{ms} + \mathbf{K}_{im}\int_0^t \mathbf{E}_{ms}dt\Big] + \mathbf{H}_{xm} - \mathbf{F}_h \tag{20}$$

where

$$\mathbf{E}_{ms} = \mathbf{X}_s - \mathbf{X}_m \tag{21}$$

and the letter *m* in the subscript representing the *master*, the diagonal matrices $\mathbf{K}_{vm}$, $\mathbf{K}_{pm}$ and $\mathbf{K}_{im}$ are the master control parameters.

B. Transparency Analysis

By combining (10) and (20), (11) and (15), the closed-loop dynamic equations can be obtained as

$$\ddot{\mathbf{X}}_s - \ddot{\mathbf{X}}_m + \mathbf{K}_{vm}(\dot{\mathbf{X}}_s - \dot{\mathbf{X}}_m) + \mathbf{K}_{pm}(\mathbf{X}_s - \mathbf{X}_m) + \mathbf{K}_{im}\int_0^t (\mathbf{X}_s - \mathbf{X}_m)dt = \mathbf{0} \tag{22}$$

for the master, and

$$\Big(\mathbf{M}_{ts}^{-1}\mathbf{K}_{ts}\mathbf{K}_{eqs}^{-1} + \mathbf{K}_{ps}\Big)\Big(\mathbf{F}_h - \mathbf{F}_e\Big) + \mathbf{K}_{is}\int_0^t \Big(\mathbf{F}_h - \mathbf{F}_e\Big)dt = \mathbf{M}_{ts}^{-1}\Big(\mathbf{M}_{ts} + \mathbf{M}_e - \mathbf{K}_{ts}\mathbf{K}_{eqs}^{-1}\mathbf{M}_e\Big)\ddot{\mathbf{X}}_s + \mathbf{M}_{ts}^{-1}\Big(\mathbf{B}_{ts} + \mathbf{B}_e - \mathbf{K}_{ts}\mathbf{K}_{eqs}^{-1}\mathbf{B}_e\Big)\dot{\mathbf{X}}_s \tag{23}$$

for the slave.

Taking Laplace transform of (22) and (23), and without loss of generality, the closed-loop dynamics can be expressed in frequency domain for a single degree of freedom as

$$(X_s - X_m)s^2 + k_{vm}(X_s - X_m)s + k_{pm}(X_s - X_m) + k_{im}(X_s - X_m)\frac{1}{s} = 0 \tag{24}$$

for the master, and

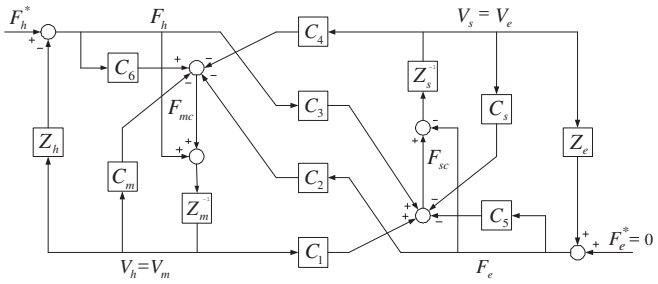

Fig. 1. Four-channel architecture with local force feedback [2].

$$\left(\frac{k_{ts}}{m_{ts}k_{eqs}} + k_{ps} + \frac{k_{is}}{s}\right)\Big(F_h - F_e\Big) = \left(1 + \frac{m_e}{m_{ts}} - \frac{m_e k_{ts}}{m_{ts}k_{eqs}}\right)s^2 X_s + \left(\frac{b_{ts}}{m_{ts}} + \frac{b_e}{m_{ts}} - \frac{b_e k_{ts}}{m_{ts}k_{eqs}}\right)sX_s \tag{25}$$

for the slave, where the parameters in small letters are the components of their corresponding matrices in (22) and (23), and X_m, X_s, F_h, and F_e are the Laplace transform of x_m, x_s, f_h, and f_e, respectively.

The four-channel architecture with local force feedback is shown in Fig. 1, from which the closed-loop dynamic equations of the master and the slave can be obtained as

$$(Z_m + C_m)V_h + C_4V_e + C_2F_e - (1 + C_6)F_h = 0 \tag{26}$$

$$(Z_s + C_s)V_e - C_1V_h - C_3F_h + (1 + C_5)F_e = 0 \tag{27}$$

Kim *et al.* [3] have derived the transparency condition of the F-P architecture as

$$\begin{cases} C_3 = 1 + C_5 \neq 0 \\ C_4 = -(Z_m + C_m) \neq 0 \\ C_6 = -1 \\ C_s = -Z_s \end{cases} \tag{28}$$

For the master, by comparing the closed-loop dynamics of the proposed master controller and the four-channel architecture, i.e., (24) and (26), one obtains

$$\begin{cases} C_4 = -(Z_m + C_m) = -\left(s^2 + k_{vm}s + k_{pm} + \frac{k_{im}}{s}\right) \neq 0 \\ C_2 = 0 \\ C_6 = -1 \end{cases} \tag{29}$$

Similarly, comparing (27) and (25) yields

$$\begin{cases} C_s + Z_s = \frac{1}{m_{ts}}\left(m_{ts} + m_e - \frac{k_{ts}}{k_{eqs}} m_e\right) s \\ \qquad\qquad + \frac{1}{m_{ts}}\left(b_{ts} + b_e - \frac{k_{ts}}{k_{eqs}} b_e\right) \\ C_3 = 1 + C_5 = \frac{k_{ts}}{m_{ts} k_{eqs}} + k_{ps} + \frac{k_{is}}{s} \\ C_1 = 0 \end{cases} \tag{30}$$

By comparing (29) and (30) with the transparency condition of the F-P architecture represented by (28), it can be seen that the perfect transparency can be achieved if $\frac{k_{ts}}{m_{ts} k_{eqs}} + k_{ps} + \frac{k_{is}}{s} \neq 0$, and

$$m_{ts} + m_e - \frac{k_{ts}}{k_{eqs}} m_e = 0 \tag{31}$$

$$b_{ts} + b_e - \frac{k_{ts}}{k_{eqs}} b_e = 0 \tag{32}$$

By substituting $k_{eqs} = k_e k_{ts}/(k_e + k_{ts})$ into (31) and (32), a simple condition set for perfect transparency can then be derived as

$$\begin{cases} \frac{k_{ts}}{m_{ts}} = \frac{k_e}{m_e}; \quad \frac{k_{ts}}{b_{ts}} = \frac{k_e}{b_e} \\ k_{pm} \neq 0 \end{cases} \tag{33}$$

Therefore, in theory, transparent teleoperation is attainable in the F-P two-channel architecture with the combined impedance/direct controller employed for the slave, and the position error based controller with local force compensation for the master, provided that the condition set (33) is satisfied. It can be shown that, if $\mathbf{K}_{im} = \mathbf{0}$, the transparency condition is the same as (33).

By observing the perfect transparency condition (33), it can be found that the force error based compensator at the slave does not contribute to the system transparency. In other words, ideally there is no difference whether the combined impedance/direct controller or the basic impedance controller is employed at the slave in terms of attainable transparency. However, in practice, un-modeled dynamics, uncertainties, and external disturbances may exist. The combined impedance/direct control is more robust to these disturbances and generates more accurate force tracking results than the basic impedance control, which has been shown in [11]. Similarly, in the discussed bilateral control system, the force error based PI-type compensator $k_{ps} + \frac{k_{is}}{s}$ in C_3 can improve the performance by rejecting the disturbances in practical situations.

Another observation is that the environment impedance is required to be known to achieve the perfect transparency. In fact, the environment impedance information has the same function as a force or position information channel, and that is why two-channel control architectures can achieve perfect transparency. It will be shown in Sec. IV that, when the environment stiffness is estimated with error, the resulted bilateral controller will produce poor force tracking results, and thus the system is not transparent.

C. Considering Transition of Motion

In the unconstrained motion, the slave robot moves in free space, and $\mathbf{Z}_e = \mathbf{0}$. Therefore, the system is transparent if the operator does not feel the force, and the slave accurately follows the motion of the master. Without the interaction between the slave and the environment, the kinematic correspondence between the master and the slave becomes the primary concern. This situation is much simpler than the constrained motion. Intuitively, the position information, rather than the force information, should be transmitted between the master and the slave. As a result, a P-P architecture is employed for unconstrained motion teleoperation. In addition, it is suggested that the force exerted by the operator to the master is compensated for, such that the feeling of force of the operator in free space is minimized. In this case, the master controller considering both constrained and unconstrained motion can be expressed as

$$\begin{aligned} \mathbf{F}_{mc} = \mathbf{D}_{xm}\Big[\ddot{\mathbf{X}}_s + \mathbf{K}_{vm}\dot{\mathbf{E}}_{ms} + \mathbf{K}_{pm}\mathbf{E}_{ms} \\ + \mathbf{K}_{im}\int_0^t \mathbf{E}_{ms} dt\Big] + \mathbf{H}_{xm} - \mathrm{sgn}(\mathbf{F}_e)\mathbf{F}_h \end{aligned} \tag{34}$$

where in this work the function $\mathrm{sgn}(\cdot)$ is defined as

$$\mathrm{sgn}(x) = \begin{cases} 1 & x > 0 \\ -1 & x = 0 \end{cases} \tag{35}$$

The slave controller maintains the same as in the constrained motion, since the combined impedance/direct control structure does not require to switch the control modes during the transition of motion. Specifically, the reference trajectory for the slave is simply set as the master position, i.e., $\mathbf{X}_r = \mathbf{X}_h$, and $\mathbf{F}_h = \mathbf{0}$. Since $\mathbf{F}_e = \mathbf{0}$ in free space motion, the slave controller is basically the impedance controller, or PD controller. Complete transparency is generally not attainable in the P-P architecture [3]. However, in the extreme situation with $\mathbf{Z}_e = \mathbf{0}$, according to Ni and Wang's result [12] about P-P architecture, we can choose high gains for the slave controller, and low gains for the master controller, such that the transmitted impedance $\mathbf{Z}_t \to \mathbf{0}$. As a result, the extreme condition for the master parameters $\mathbf{K}_{vm} = \mathbf{K}_{pm} = \mathbf{K}_{im} = \mathbf{0}$ is set for the unconstrained motion. Therefore, the same controllers for both the master and the slave as in the constrained motion are used in the unconstrained motion.

The transition of motion between the unconstrained and constrained conditions is common during most manipulation tasks. The proposed bilateral controller requires no control mode switch of both the master and the slave controllers during the transition of motion. Once the designed controllers are implemented, they can work in both the constrained and unconstrained conditions. The only difference between

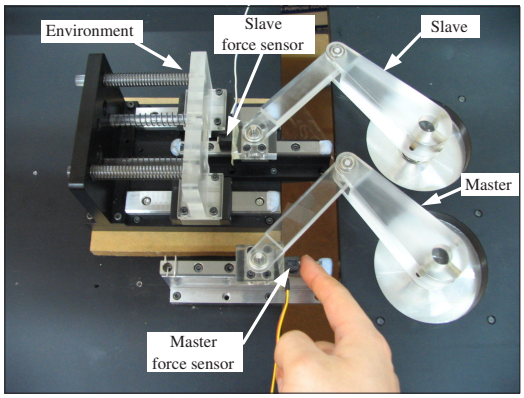

Fig. 2. Teleoperation experimental platform.

the constrained and unconstrained conditions is that different communication channels are used. The values of the control parameters $\mathbf{K}_{ts}$, $\mathbf{K}_{pm}$, $\mathbf{K}_{vm}$ and $\mathbf{K}_{im}$ need to be switched when the transition of motion takes place, in order to achieve the perfect transparency. In fact, the value of $\mathbf{K}_{ts}$ can be remained unchanged for both constrained and unconstrained motions.

IV. Experiments

The experiments are conducted on a system with two identical single degree of freedom slider crank mechanisms. Note that the operator is one of the authors. The experiments are designed to study and evaluate the performance of the proposed controller.

A. Experimental Platform

Figure 2 shows the photograph of the constructed platform. Both the master and the slave are driven by the Emoteq^{TM} direct drive brushless DC motors (QB03400) with the continuous torque up to 0.81 Nm. The encoders with 2000 pulses per revolution are mounted at the end of the motor shafts to measure the angular position. The AMC^{TM} servo amplifiers (B15A) are used to output current commands to the motors. Two simple Honeywell^{TM} one-axis force sensor (FSG15N1A) are attached on the master and the slave, respectively, which are connected to an amplifier circuit to measure the interaction force. The Sensoray^{TM} I/O board (Model 626) is used to read the sensor readings and to output commands to the motors through the amplifiers. The xPC Target toolbox of Matlab^{TM} is used to implement the control system with the sampling frequency at 1 kHz. Detailed software implementation can be found in [13].

Without considering the Coulomb and viscous frictions, the dynamic equation (of both the master and the slave) can be obtained as

$$d(q)\ddot{q} + c(q)\dot{q} = \tau \tag{36}$$

where the parameters are estimated to be $d(q) = \left(7.10\cos^2 q + 2.58\right) \times 10^{-4}$ kgm^2, and $c(q) = 3.55 \times 10^{-4}\dot{q}\sin(2q)$ kgm^2/s. Note that there are errors between

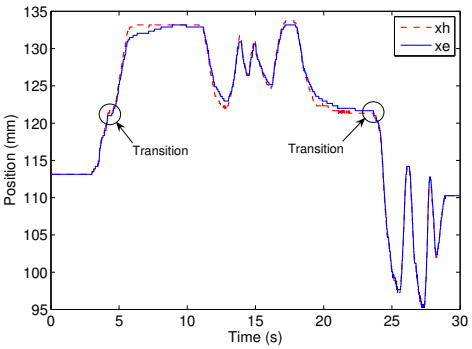

(a) Position

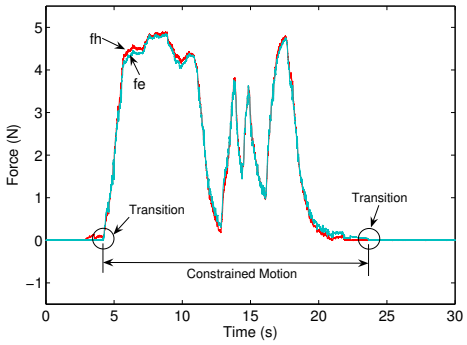

(b) Force

Fig. 3. Results of a typical operation including transition between the free space motion and the constrained motion. (k_e and m_e are known, and b_e is unknown.)

the estimations and the real values. The environment adopts a mass-damper-spring system, which consists of a moving plate mounted on two sliders, and several spring components. The values of the impedance parameters are $m_e = 0.14$ kg, $k_e = 400$N/m, and b_e is small and unknown. The acceleration term is dropped from the master controller in the experiments.

B. Experimental Results

In the experiment, the slave slider initially locates at $x = 113.10$. So does the master slider. During the experiment, the operator pushes the master slider along the x-axis direction. When the slave slider contacts the environment at $x = 122.32$, the free space motion transits to the constrained motion. Afterwards, the operator repeats to push and then release the master several times, followed by the transition from the constrained motion to the free space motion.

In the experiment, the parameters are set as $k_{ps} = 90$, $k_{is} = 80$, $m_{ts} = 1$, $b_{ts} = 10$, and $k_{ts} = 1.8 \times 10^4$ (all the parameters and variables are in SI units, which are omitted for simplicity). During the constrained motion, the parameters of the master controller are set as $k_{pm} = 1.8 \times 10^4$, $k_{vm} = 10$, and $k_{im} = 10^4$. While during the unconstrained motion, $k_{pm} = k_{vm} = k_{im} = 0$. During the transition of motion, the control modes and the values of the control parameters of the slave controller are not switched. For the master, the control mode is also kept un-switched, while the values of the control parameters should

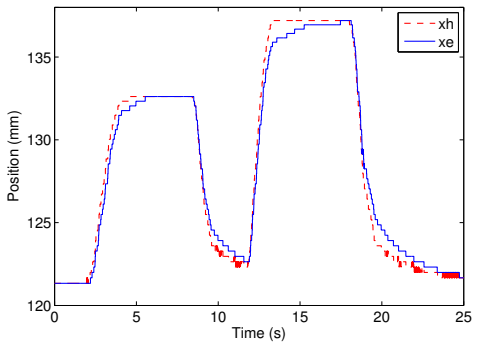

(a) Position

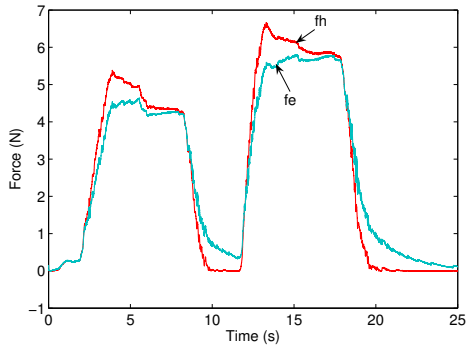

(b) Force

Fig. 4. Results in the case that the environment stiffness is estimated with error. (m_e is known, and k_e and b_e are unknown. k_e is estimated as $\hat{k}_e = 2500$ N/m.)

be switched from $k_{pm} = k_{vm} = k_{im} = 0$ to $k_{pm} = 1.8 \times 10^4$, $k_{vm} = 10$, and $k_{im} = 10^4$ when the motion transits from the free space to the constrained condition, and vice versa.

As shown in Fig. 3, the motion transits smoothly, and the force and position between the master and the slave are well matched. In addition, the kinematic correspondence is maintained when the motion transits from the contact condition to the free space, which is important for repetitive and consecutive manipulations. High transparency in both constrained and unconstrained motions has now been demonstrated by the results.

It is then assumed that the environment stiffness is unknown and estimated to be $\hat{k}_e = 2500$. The slave target stiffness is thus designed to be $k_{ts} = 1.8 \times 10^4$ according to (33), in order to achieve perfect transparency. Figure 4 shows the results in constrained motion. The force tracking performance deteriorates drastically. The results comply with the analysis in Sec. III-B that for the F-P two channel control architecture, the information of the environment impedance is required to be known to achieve perfect transparency.

V. Concluding Remarks

The proposed bilateral control scheme has the following features. Firstly, perfect transparency can be achieved in the two-channel control architecture. Secondly, due to the disturbance rejection capability of the combined impedance/direct control, $\mathbf{F}_e$ can be controlled with high accuracy with the presence of robot dynamic uncertainties and external disturbances. Thirdly, although different control architectures are employed for the constrained and unconstrained motions, it dose not need to switch the control modes of the master and the slave controllers during the transition of motion. Once the designed controllers are implemented, they can work in both the constrained and unconstrained conditions. The only difference between the constrained and unconstrained conditions is that different communication channels are used.

The experimental results in Sec. IV were obtained based on one subject only. The performance by different subjects will be considered in the future study. Furthermore, the acceleration term of the proposed controller will be included in the future experimental study.

References

[1] D. A. Lawrence, "Stability and transparency in bilateral teleoperation," *IEEE Transactions on Robotics and Automation*, vol. 9, no. 5, pp. 624–637, 1993.

[2] K. Hashtrudi-Zaad and S. E. Salcudean, "Transparency in time-delayed systems and th effect of local force feedback for transparent teleoperation," *IEEE Transactions on Robotics and Automation*, vol. 18, no. 1, pp. 108–114, 2002.

[3] J. Kim, P. H. Chang, and H.-S. Park, "Transparent teleoperation using two-channel control architectures," *in Proceedings of the IEEE International Conference on Intelligent Robots and Systems (IROS'05)*, Edmonton, Alberta, Canada, Aug. 2005, pp. 2824-2831.

[4] K. B. Fite, L. Shao, and M. Goldfarb, "Loop shaping for transparency and stability robustness in bilateral telemanipulation," *IEEE Transactions on Robotics and Automation*, vol. 20, no. 3, pp. 620–624, 2004.

[5] K. B. Fite, J. E. Speich, and M. Goldfarb, "Transparency and stability robustness in two-channel bilateral telemanipulation," *Journal of dynamic Systems, Measurement, and Control*, vol. 123, no. 3, pp. 400–407, 2001.

[6] F. Aghili, E. Dupuis, E. Martin, and J-C. Piedboeuf, "Force/moment accommodation control for tele-operated manipulators performing contact tasks in stiff environment," *in Proceedings of the IEEE International Conference on Intelligient Robots and Systems (IROS'01)*, Maui, Hawaii, USA, Oct-Nov. 2001, pp. 2227–2233.

[7] R. L. Williams II, J. M. Henry, and M. A. Murphy, "Free and constrained motion teleoperation via Naturally-Transitioning Rate-to-Force Control," *in Proceedings of the IEEE International Conference on Robotics and Automation (ICRA'99)*, Detroit, Michigan, May 1999, pp. 225–230.

[8] R. L. Williams II, J. M. Henry, and D. W. Repperger, "Evaluation of rate-based, force-reflecting teleoperation in free motion and contact," *Presence*, vol. 9, no. 1, pp. 25–36, 2000.

[9] S. Jung, T. C. Hsia, and R. G. Bonitz, "Force tracking impedance control for robot manipulators with an unknown environment: Theory, simulation, and experiment," *The International Journal of Robotics Research*, vol. 20, no. 9, pp. 765–774, 2001.

[10] H. Wang, K. H. Low, and M. Y. Wang, "On the position/force control of robotic manipulators with model uncertainty and random disturbances," *in Proceedings of the IEEE International Conference on Robotics and Mechatronics (RAM'06)*, Bangkok, Thailand, June 2006, pp. 134–139.

[11] H. Wang, K. H. Low, and M. Y. Wang, "Combined impedance/direct control of robot manipualtors," *in Proceedings of the IEEE International Conference on Intelligient Robots and Systems (IROS'06)*, Beijing, China, Oct. 2006.

[12] L. Ni and W. L. Wang, "A gain-switching control scheme for position-error-based bilateral teleoperation system: Contact stability analysis and controller design," *The International Journal of Robotics Research*, vol. 23, no. 3, pp. 255–274, 2004.

[13] K. H. Low, H. Wang, K. M. Liew, and Y. Cai, "Modeling and motion control of robotic hand for telemanipulation application," *International Journal of Software Engineering and Knowledge Engineering*, vol. 15, no. 2, pp. 147–152, 2005.